CLNS 07/1995
CLEO 07-05

Search for Radiative Decays of $\Upsilon(1S)$ into η and η'

S. B. Athar,[1] R. Patel,[1] V. Potlia,[1] H. Stoeck,[1] J. Yelton,[1] P. Rubin,[2] C. Cawlfield,[3] B. I. Eisenstein,[3] I. Karliner,[3] D. Kim,[3] N. Lowrey,[3] P. Naik,[3] C. Sedlack,[3] M. Selen,[3] E. J. White,[3] J. Wiss,[3] M. R. Shepherd,[4] D. Besson,[5] T. K. Pedlar,[6] D. Cronin-Hennessy,[7] K. Y. Gao,[7] D. T. Gong,[7] J. Hietala,[7] Y. Kubota,[7] T. Klein,[7] B. W. Lang,[7] R. Poling,[7] A. W. Scott,[7] A. Smith,[7] S. Dobbs,[8] Z. Metreveli,[8] K. K. Seth,[8] A. Tomaradze,[8] P. Zweber,[8] J. Ernst,[9] H. Severini,[10] S. A. Dytman,[11] W. Love,[11] V. Savinov,[11] O. Aquines,[12] Z. Li,[12] A. Lopez,[12] S. Mehrabyan,[12] H. Mendez,[12] J. Ramirez,[12] G. S. Huang,[13] D. H. Miller,[13] V. Pavlunin,[13] B. Sanghi,[13] I. P. J. Shipsey,[13] B. Xin,[13] G. S. Adams,[14] M. Anderson,[14] J. P. Cummings,[14] I. Danko,[14] J. Napolitano,[14] Q. He,[15] J. Insler,[15] H. Muramatsu,[15] C. S. Park,[15] E. H. Thorndike,[15] T. E. Coan,[16] Y. S. Gao,[16] F. Liu,[16] M. Artuso,[17] S. Blusk,[17] J. Butt,[17] J. Li,[17] N. Menaa,[17] R. Mountain,[17] S. Nisar,[17] K. Randrianarivony,[17] R. Redjimi,[17] R. Sia,[17] T. Skwarnicki,[17] S. Stone,[17] J. C. Wang,[17] K. Zhang,[17] S. E. Csorna,[18] G. Bonvicini,[19] D. Cinabro,[19] M. Dubrovin,[19] A. Lincoln,[19] D. M. Asner,[20] K. W. Edwards,[20] R. A. Briere,[21] I. Brock,[21] J. Chen,[21] T. Ferguson,[21] G. Tatishvili,[21] H. Vogel,[21] M. E. Watkins,[21] J. L. Rosner,[22] N. E. Adam,[23] J. P. Alexander,[23] K. Berkelman,[23] D. G. Cassel,[23] J. E. Duboscq,[23] K. M. Ecklund,[23] R. Ehrlich,[23] L. Fields,[23] R. S. Galik,[23] L. Gibbons,[23] R. Gray,[23] S. W. Gray,[23] D. L. Hartill,[23] B. K. Heltsley,[23] D. Hertz,[23] C. D. Jones,[23] J. Kandaswamy,[23] D. L. Kreinick,[23] V. E. Kuznetsov,[23] H. Mahlke-Krüger,[23] T. O. Meyer,[23] P. U. E. Onyisi,[23] J. R. Patterson,[23] D. Peterson,[23] J. Pivarski,[23] D. Riley,[23] A. Ryd,[23] A. J. Sadoff,[23] H. Schwarthoff,[23] X. Shi,[23] S. Stroiney,[23] W. M. Sun,[23] T. Wilksen,[23] and M. Weinberger[23]

(CLEO Collaboration)

[1]*University of Florida, Gainesville, Florida 32611*
[2]*George Mason University, Fairfax, Virginia 22030*
[3]*University of Illinois, Urbana-Champaign, Illinois 61801*
[4]*Indiana University, Bloomington, Indiana 47405*
[5]*University of Kansas, Lawrence, Kansas 66045*
[6]*Luther College, Decorah, Iowa 52101*
[7]*University of Minnesota, Minneapolis, Minnesota 55455*
[8]*Northwestern University, Evanston, Illinois 60208*
[9]*State University of New York at Albany, Albany, New York 12222*
[10]*University of Oklahoma, Norman, Oklahoma 73019*
[11]*University of Pittsburgh, Pittsburgh, Pennsylvania 15260*
[12]*University of Puerto Rico, Mayaguez, Puerto Rico 00681*
[13]*Purdue University, West Lafayette, Indiana 47907*
[14]*Rensselaer Polytechnic Institute, Troy, New York 12180*
[15]*University of Rochester, Rochester, New York 14627*
[16]*Southern Methodist University, Dallas, Texas 75275*
[17]*Syracuse University, Syracuse, New York 13244*
[18]*Vanderbilt University, Nashville, Tennessee 37235*
[19]*Wayne State University, Detroit, Michigan 48202*
[20]*Carleton University, Ottawa, Ontario, Canada K1S 5B6*
[21]*Carnegie Mellon University, Pittsburgh, Pennsylvania 15213*

[22]*Enrico Fermi Institute, University of Chicago, Chicago, Illinois 60637*
[23]*Cornell University, Ithaca, New York 14853*
(Dated: April 19, 2007)

Abstract

We report on a search for the radiative decay of $\Upsilon(1S)$ to the pseudoscalar mesons η and η' in $(21.2 \pm 0.2) \times 10^6$ $\Upsilon(1S)$ decays collected with the CLEO III detector at the Cornell Electron Storage Ring (CESR). The η meson was reconstructed in the three modes $\eta \to \gamma\gamma$, $\eta \to \pi^+\pi^-\pi^0$ or $\eta \to \pi^0\pi^0\pi^0$. The η' meson was reconstructed in the mode $\eta' \to \pi^+\pi^-\eta$ with η decaying through any of the above three modes, and also $\eta' \to \gamma\rho^0$, where $\rho^0 \to \pi^+\pi^-$.

Five out of the seven sub-modes are found to be virtually background-free. In four of them we find no signal candidates and in one $(\Upsilon(1S) \to \gamma\eta',\ \eta' \to \pi^+\pi^-\eta,\ \eta \to \pi^+\pi^-\pi^0)$

there are two good signal candidates, which is insufficient evidence to claim a signal.

The other two sub-modes ($\eta \to \gamma\gamma$ and $\eta' \to \gamma\rho^0$) are background limited, and show no excess of events in their signal regions. We combine the results from different channels and obtain upper limits at the 90% C.L. which are $\mathcal{B}(\Upsilon(1S) \to \gamma\eta) < 1.0 \times 10^{-6}$ and $\mathcal{B}(\Upsilon(1S) \to \gamma\eta') < 1.9 \times 10^{-6}$. Our limits are an order of magnitude tighter than the previous ones and below the predictions made by some theoretical models.

I. INTRODUCTION

The hadronic decays of heavy quarkonia below the threshold for heavy meson pair production are understood to proceed predominantly via three intermediate gluons. One of the gluons can be replaced by a photon with a penalty of order the ratio of coupling constants, α/α_s. Such exclusive radiative decays of the heavy vector mesons J/ψ and Υ have been the subject of many experimental and theoretical studies. For the experimenter, the final states from radiative decays are relatively easy to identify as they have a high energy photon, a low multiplicity of other particles, and low background. Theoretically, the radiative decays of heavy quarkonia into a single light hadron provide a particularly clean environment to study the conversion of gluons into hadrons, and thus their study is a direct test of QCD. $\Upsilon(1S) \to \gamma\eta'$ is one such candidate channel. This decay channel has been observed to be produced in the J/ψ charmonium system (the 1^3S_1 state of $c\bar{c}$) with $\mathcal{B}(J/\psi \to \gamma\eta') = (4.71 \pm 0.27) \times 10^{-3}$ [1]. Naive scaling predicts that decay rates for radiative $\Upsilon(1S)$ decays are suppressed by the factor $(q_b m_c/q_c m_b)^2 \approx 1/40$ with respect to the corresponding J/ψ radiative decays. This factor arises because the quark-photon coupling is proportional to the electric charge, and the quark propagator is roughly proportional to $1/m$ for low momentum quarks. Taking into account the total widths [1] of J/ψ and $\Upsilon(1S)$, the branching fraction of a particular $\Upsilon(1S)$ radiative decay mode is expected to be around 0.04 of the corresponding J/ψ branching fraction. However, the CLEO search [2] for $\Upsilon(1S) \to \gamma\eta'$ in $61.3\,\mathrm{pb}^{-1}$ of data collected with the CLEO II detector found no signal in this mode, and resulted in a 90% confidence level upper limit of 1.6×10^{-5} for the branching fraction $\Upsilon(1S) \to \gamma\eta'$, an order of magnitude smaller than this expectation.

The two-body decay $\Upsilon(1S) \to \gamma f_2(1270)$ has been observed [3] in the older CLEO II $\Upsilon(1S)$ analysis, and this observation has been confirmed [4, 5], with much greater statistics, in CLEO III data. The measurement $\mathcal{B}(\Upsilon(1S) \to \gamma f_2(1270)) = (10.2 \pm 1.0) \times 10^{-5}$, from the combination of the two CLEO III measurements, is 0.074 ± 0.010 times the corresponding J/ψ decay mode, showing a deviation of roughly a factor of two from the naive scaling estimates. In radiative J/ψ decays the ratio of η' to $f_2(1270)$ production is 3.4 ± 0.4. If the same ratio held in $\Upsilon(1S)$, the η' channel would be clearly visible. The channel $\Upsilon(1S) \to \gamma\eta$ has received significant theoretical attention. This channel has been observed in J/ψ decays [1] with the branching fraction of $(9.8 \pm 1.0) \times 10^{-4}$, a value smaller by a factor of five than $\mathcal{B}(J/\psi \to \gamma\eta')$. The previous CLEO search of $\Upsilon(1S)$ decays produced an upper limit of 2.1×10^{-5} at the 90% confidence level for this mode [6].

Several authors have tried to explain the lack of signals in radiative $\Upsilon(1S)$ decays into pseudoscalar mesons, using a variety of models which produce branching fraction predictions of 10^{-6} to 10^{-4}. Employing the Vector Meson Dominance Model (VDM), Intemann [7] predicts the branching fractions for the heavy vector meson radiative decay into light pseudoscalar mesons. Using the mixing mechanism of η, η' with the as-yet-unobserved pseudoscalar resonance η_b, Chao [8] first calculated the mixing angle $\lambda_{\eta\eta_b}$ in order to estimate the radiative branching fractions. Baier and Grozin [9] showed that for light vector mesons (such as J/ψ) there might be an additional "anomaly" diagram that contributes significantly to the radiative decays. Noting that VDM has no direct relation to QCD as the fundamental theory of strong interactions, and referring to [7], Ma tries to address the problem by using factorization at tree level with NRQCD matrix elements to describe the heavy vector meson portion multiplied by a set of twist-2 and twist-3 gluonic distribution amplitudes [10].

II. DETECTOR AND DATA SAMPLE

This study is based upon data collected by the CLEO III detector at the Cornell Electron Storage Ring (CESR). CLEO III is a versatile multi-purpose particle detector described fully elsewhere [11]. Centered on the e^+e^- interaction region of CESR, the inner detector consists of a silicon strip vertex detector and a wire drift chamber measuring the momentum vectors and the ionization energy losses (dE/dx) of charged tracks based on their trajectories in the presence of a 1.5T solenoidal magnetic field. The silicon vertex detector and the drift chamber tracking system together achieve a charged particle momentum resolution of 0.35% (1%) at $1\,\mathrm{GeV}/c$ ($5\,\mathrm{GeV}/c$) and a fractional dE/dx resolution of 6% for hadrons and 5% for electrons. Beyond the drift chamber is a Ring Imaging Cherenkov Detector, RICH, which covers 80% of the solid angle and is used to further identify charged particles by giving for each mass hypothesis the fit likelihood to the measured Cherenkov radiation pattern. After the RICH is a CsI crystal calorimeter that covers 93% of the solid angle, allowing both photon detection and electron suppression. The calorimeter provides an energy resolution of 2.2% (1.5%) for 1 GeV (5 GeV) photons. Beyond the calorimeter is a superconducting solenoidal coil providing the magnetic field, followed by iron flux return plates with wire chambers interspersed at 3, 5, and 7 hadronic interaction lengths (at normal incidence) to provide muon identification.

The data sample has an integrated luminosity of $1.13\,\mathrm{fb}^{-1}$ taken at the $\Upsilon(1\mathrm{S})$ energy $\sqrt{s} = 9.46$ GeV, which corresponds to $N_{\Upsilon(1\mathrm{S})} = 21.2 \pm 0.2$ million $\Upsilon(1\mathrm{S})$ decays [12]. The efficiencies for decay chain reconstruction were obtained from Monte Carlo simulated radiative events generated with the $(1 + \cos^2\theta)$ angular distribution expected for decays $\Upsilon(1\mathrm{S}) \to \gamma + \mathrm{pseudoscalar}$. The Monte Carlo simulation of the detector response was based upon GEANT [13], and simulation events were processed in an identical fashion to data.

III. EVENT SELECTION AND RESULTS

In our search for $\Upsilon(1\mathrm{S}) \to \gamma\eta$ and $\Upsilon(1\mathrm{S}) \to \gamma\eta'$, we reconstruct η mesons in the modes $\eta \to \gamma\gamma$, $\eta \to \pi^+\pi^-\pi^0$, and $\eta \to \pi^0\pi^0\pi^0$; the latter two will collectively be referred to as $\eta \to 3\pi$. We reconstruct the η' meson in the mode $\eta\pi^+\pi^-$ with η decaying in any of the above modes, and in addition, the mode $\eta' \to \gamma\rho^0$, where $\rho^0 \to \pi^+\pi^-$. From the CLEO II studies [2, 6] we expected five out of the seven modes under investigation to be relatively background free and so we employ minimal selection criteria to maximize sensitivity and minimize possible systematic biases. The other two, $\eta \to \gamma\gamma$ and $\eta' \to \gamma\rho^0$, have large branching fractions, but also large backgrounds, and so our event selection for these modes aims to decrease the background with a corresponding loss of efficiency.

Our general analysis strategy is to reconstruct the complete decay chain ensuring that none of the constituent tracks or showers have been used more than once, then kinematically constrain the intermediate π^0 and η meson candidates to their nominal masses [1], and finally require the event to be consistent with having the 4-momentum of the initial e^+e^- system. Multiply-reconstructed $\Upsilon(1\mathrm{S})$ candidates in an event, a problem of varying severity from mode to mode, is dealt with by selecting the combination with lowest χ^2_{Total}, the sum of chi-squared of the 4-momentum constraint (χ^2_{P4}) and chi-squared of all the mass-constraints involved in a particular decay chain. For example, there are four mass-constraints involved in the decay chain $\Upsilon(1\mathrm{S}) \to \gamma\eta'; \eta \to \pi^0\pi^0\pi^0$, three π^0 mass-constraints and one η mass-constraint. The mode $\Upsilon(1\mathrm{S}) \to \gamma\eta; \eta \to \pi^0\pi^0\pi^0$ is an exception in which we preferred to accept the $\eta \to \pi^0\pi^0\pi^0$ candidate having the lowest $S_\pi^2 \equiv \sum_i^3 S_{\pi,i}^2$, with $S_{\pi,i} \equiv (m_{\gamma\gamma} - m_{\pi^0})/\sigma_{\gamma\gamma}$ of the ith π^0candidate. The yield is obtained by counting the number of final state η or η' candidates within our acceptance mass window defined as the invariant mass region centered around the mean value and providing 98% signal acceptance as determined from signal Monte Carlo. Whenever possible, an event vertex is calculated using the information from the charged tracks, and the 4-momentum of the photon candidates is then recalculated, assuming that the showers originate from the event vertex rather than the origin of the CLEO coordinate system. This produces an improvement in the η and η' candidates' invariant mass resolution of roughly 10%, leading to a slight increase in the sensitivity of the measurement.

The CLEO III trigger [14] relies upon two components: (1) the tracking-based "axial" and "stereo" triggers derived from the signals on the 16 axial layers of the drift chamber, and the signals registered on the chamber's 31 stereo layers, and (2) the calorimeter-based trigger derived from the energy deposition in the CsI crystal calorimeter. The events for the "all neutral" modes $\Upsilon(1S) \to \gamma\eta; \eta \to \gamma\gamma$ and $\Upsilon(1S) \to \gamma\eta; \eta \to \pi^0\pi^0\pi^0$ are collected by the calorimeter-based trigger condition requiring two high energy back-to-back showers. We demand that triggered events meet the following analysis requirements: (a) a high energy calorimeter shower not associated with a charged track, having a lateral profile consistent with being a photon, and having a measured energy greater than 4.0 GeV must be present; (b) there must be the correct number of pairs of oppositely charged, good quality tracks with usable dE/dx information. The efficiency of these requirements is more than 60% in modes involving charged tracks and approximately 54% and 45% for cases where $\eta \to \gamma\gamma$ and $\eta \to 3\pi^0$, respectively.

The photon candidates we use in forming π^0 and $\eta \to \gamma\gamma$ candidates have minimum energy depositions of 30 MeV and 50 MeV, respectively. All photon candidates are required to be not associated to charged tracks, and at least one of the photon candidates of each pair must have a lateral profile consistent with that expected for a photon. The photon candidates we use in reconstructing the η meson in the $\gamma\gamma$ mode must be detected either in the fiducial barrel or the fiducial endcap[1] calorimeter region only. These candidates are then kinematically constrained to the nominal meson mass, the exception being $\Upsilon(1S) \to \gamma\eta; \eta \to \gamma\gamma$, where no mass-constraining was done to the η candidate, because we examine $m_{\gamma\gamma}$ in this mode to determine our yield.

The η candidates in the mode $\pi^+\pi^-\pi^0$ are built by first forcing pairs of oppositely charged quality tracks to originate from a common vertex. The π^0 candidate having invariant mass within $7\sigma_{\gamma\gamma}$ is then added to complete the reconstruction of $\eta \to \pi^+\pi^-\pi^0$ candidates. The charged tracks are required to be consistent with being pions by adding the pion hypothesis $\mathrm{S}_{dE/dx} \equiv (dE/dx(\text{measured}) - dE/dx(\text{expected}))/\sigma_{dE/dx}$ in quadrature for two tracks and requiring the sum of $\mathrm{S}^2_{dE/dx}$ to be less than 16.

In the case of $\eta \to \pi^0\pi^0\pi^0$, the η candidate is simply built by adding three different π^0 candidates, where no constituent photon candidate contributes more than once in a candidate $\eta \to \pi^0\pi^0\pi^0$ reconstruction. The π^0 candidates are selected by requiring $S_\pi < 10.0$. In order to increase the efficiency in this mode, an exception was made to the fiducial region requirement, and photons in the gap between the barrel and endcap fiducial regions were

[1] The fiducial regions of the barrel and endcap are defined by $|\cos(\theta)| < 0.78$ and $0.85 < |\cos(\theta)| < 0.95$, respectively; the region between the barrel fiducial region and the endcap fiducial region is not used due to its relatively poor resolution.

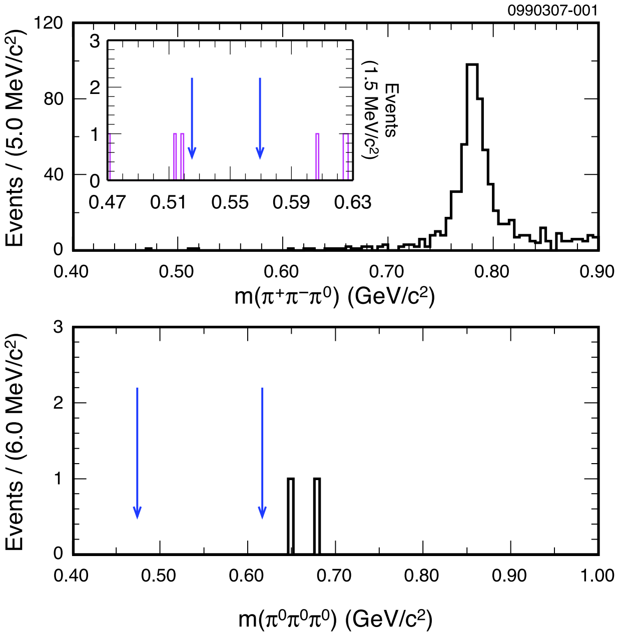

FIG. 1: Candidate $\eta \to \pi^+\pi^-\pi^0$ (top) and $\eta \to \pi^0\pi^0\pi^0$ (bottom) invariant mass distributions from Υ(1S) data. The large number of events near 780 MeV/c^2 (top) is due to the abundant process $e^+e^- \to \gamma\omega$. No events are observed in our acceptance region, bounded by the arrows.

allowed.

A. The Decay $\Upsilon \to \gamma\eta, \eta \to 3\pi$

The Υ candidate in the mode $\gamma\eta$ is formed by combining a high-energy photon ($E >$ 4 GeV) with the η candidate, requiring that this photon is not a daughter of the η candidate. The Υ candidate is then subjected to the 4-momentum constraint of the initial e^+e^- system. In the case of $\eta \to 3\pi$, multiply reconstructed Υ candidates were restricted by selecting only one candidate. For $\eta \to \pi^+\pi^-\pi^0$, we select the candidate with the lowest χ^2_{Total}, the sum of chi-squared of the 4-momentum constraint and chi-squared of the mass-constraint to the π^0 candidate. For $\eta \to \pi^0\pi^0\pi^0$, we select the candidate with the smallest S^2_π. The selected Υ candidate is further required to satisfy the 4-momentum consistency criterion, restricting $\chi^2_{\mathrm{P4}} < 100$ for $\eta \to \pi^+\pi^-\pi^0$ and a less stringent cut of 200 for $\eta \to \pi^0\pi^0\pi^0$ measurements. In addition, we limit the number of reconstructed calorimeter showers for the mode $\Upsilon(1S) \to \gamma\eta; \eta \to \pi^0\pi^0\pi^0$ to minimize backgrounds such as $e^+e^- \to \gamma\phi$ where $\phi \to K_S K_L$ without jeopardizing the signal efficiency.

From Monte Carlo simulations, the overall reconstruction efficiencies, ϵ_i, for each channel are determined to be $(28.5 \pm 4.3)\%$ and $(11.8 \pm 1.9)\%$ for the decay chains $\Upsilon \to \gamma\eta, \eta \to \pi^+\pi^-\pi^0$ and $\Upsilon \to \gamma\eta, \eta \to \pi^0\pi^0\pi^0$, respectively. The uncertainties in the efficiency include the Monte Carlo samples' statistical uncertainty and our estimate of possible systematic biases, which are discussed further in Section IV.

We find no candidate events within our acceptance invariant mass window for the search $\Upsilon(1S) \to \gamma\eta$, $\eta \to 3\pi$. The invariant mass distributions for candidate $\eta \to \pi^+\pi^-\pi^0$ and $\eta \to \pi^0\pi^0\pi^0$, after imposing all the selection criteria are shown in Figure 1.

B. The Decay $\Upsilon \to \gamma\eta, \eta \to \gamma\gamma$

The 3-photon final state resulting from $\Upsilon(1S) \to \gamma\eta; \eta \to \gamma\gamma$ is dominated by the QED process $e^+e^- \to \gamma\gamma\gamma$. Our selection criteria of loosely reconstructing an $\eta \to \gamma\gamma$ meson and requiring the χ^2 of 4-momentum constraint on the $\Upsilon(1S)$ meson formed by adding a hard-photon to be < 200 are not sufficient to suppress this background. The QED background, however has a distinct feature - the two photons having energies E_{hi} and E_{lo} used in reconstructing the η candidate have a large energy asymmetry, where asymmetry is defined as $(E_{hi} - E_{lo})/(E_{hi} + E_{lo})$. Real η mesons are expected to have an approximately uniform distribution of asymmetry in the range (0,1). We require the asymmetry to be less than 0.8. To further discriminate between the signal and the background, we used a neural net approach.

The input to the neural net is a vector of six variables, namely the measured energy and the polar angle θ of each of the three calorimeter showers used in the reconstruction chain. The training sample is comprised of 20,000 simulated signal and background events in equal proportion. The simulated $e^+e^- \to \gamma\gamma\gamma$ background events have a high-energy photon ($E > 4$ GeV), $\gamma\gamma$ invariant mass for the two lower-energy photons in the range 0.4-0.7 GeV/c^2, and energy asymmetry less than 0.8.

For our final selection, we choose neural-net output with 51% efficiency while rejecting 86% of the background. The combined efficiency of our selection criteria for this mode is $(23.8 \pm 2.4)\%$, which includes possible systematic biases and statistical uncertainties from the simulation. The resulting $\gamma\gamma$ invariant mass distribution from $\Upsilon(1S)$ data is fit, as shown in Figure 2, to a double Gaussian function, whose mass and widths are fixed to values found from signal Monte Carlo data, along with a second order polynomial background function. From this likelihood fit, we obtain -2.3 ± 8.7 events; consistent with zero. We then perform the same likelihood fit multiple times fixing the signal area to different values, assigning each of the fits a probability proportional to $e^{-\chi^2/2}$, where χ^2 is obtained from the likelihood fit. The resulting probability distribution is normalized and numerically integrated up to 90% of the area to obtain the yield at 90% confidence level. Our limit thus obtained is 14.5 events at 90% confidence level.

C. The Decay $\Upsilon \to \gamma\eta', \eta' \to \eta\pi^+\pi^-$

Reconstruction of the decay chains $\Upsilon(1S) \to \gamma\eta'$, where $\eta' \to \eta\pi^+\pi^-$, builds on the search $\Upsilon(1S) \to \gamma\eta$The reconstructed η candidate is constrained to the nominal η mass. The mass-constrained η candidate is further combined with a pair of oppositely charged quality tracks by forcing the tracks and the η candidate to originate from a common vertex. In reconstruction of $\eta'; \eta \to \pi^+\pi^-\pi^0$, care is exercised to ensure that no track is used more than once in the decay chain. The high energy photon is combined with the η' candidate to build an Υ candidate which is further constrained to the 4-momentum of the initial e^+e^- system. In the reconstruction chain $\eta'; \eta \to \gamma\gamma$, the Υ candidate with the lowest sum of chi-squared to the 4-momentum constraint (χ^2_{P4}) combined with the chi-squared of the mass-constraint to the η candidate (χ^2_η) is accepted as the representative Υ candidate in the reconstructed event. In the modes where $\eta \to 3\pi$, the π^0 mass-constraint chi-squared, $\chi^2_{\pi^0}$, also contributes to the χ^2_{Total}.

To ensure that only good quality η candidates participate in the decay chain, the χ^2_η values of "$\eta \to$ all neutral" candidates are required to be less than 200. Owing to the better

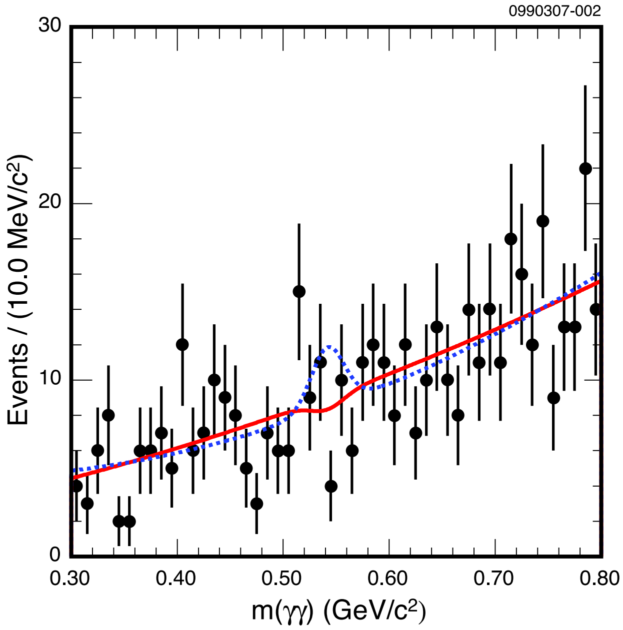

FIG. 2: Invariant mass distribution of $\gamma\gamma$ candidates in $\Upsilon(1S)$ data for the mode $\Upsilon(1S) \to \gamma\eta; \eta \to \gamma\gamma$, overlaid with fits using a) floating area (solid red) yielding -2.3 ± 8.7 events, and b) area fixed to 14.5 events (dashed blue), the upper limit corresponding to 90% C.L.

measurements of charged track momenta, this criterion is more stringent ($\chi^2_\eta < 100$) in the case of $\eta \to \pi^+\pi^-\pi^0$. The targeted efficiency (around 99%) of this requirement is achieved in all three cases.

The charged tracks used in reconstructing η' candidates have to be consistent with the pion hypothesis. We again require the sum of squared $S_{dE/dx}$ added in quadrature to be less than 16 for both the two track and four track cases. The efficiency of this requirement alone is around 99%.

The selected Υ candidate is further required to satisfy the 4-momentum consistency criterion, restricting $\chi^2_{\rm P4} < 100$ in the $\eta \to \gamma\gamma$ case and a less stringent value of 200 for $\eta \to 3\pi$. The overall reconstruction efficiencies of our selection criteria as determined from signal Monte Carlo simulations are $(35.3 \pm 5.2)\%$, $(24.5 \pm 2.2)\%$ and $(14.4 \pm 2.9)\%$ for η decays to $\gamma\gamma$, $\pi^+\pi^-\pi^0$ and $3\pi^0$, respectively.

After these selection criteria, we find no candidate events in the modes $\Upsilon(1S) \to \gamma\eta'; \eta \to \gamma\gamma$ and $\Upsilon(1S) \to \gamma\eta'; \eta \to \pi^0\pi^0\pi^0$, as shown in Figure 3. However, in the mode $\Upsilon(1S) \to \gamma\eta'; \eta \to \pi^+\pi^-\pi^0$, we find two good candidate events passing our selection criteria as shown in Figure 3. These two events have been looked at in detail and appear to be good signal events. However, they are insufficient to allow us to claim a positive signal, as no candidate events are observed in the modes $\Upsilon(1S) \to \gamma\eta'; \eta \to \gamma\gamma$ and $\Upsilon(1S) \to \gamma\eta'; \eta \to \pi^0\pi^0\pi^0$, each providing higher sensitivity than the decay chain $\Upsilon(1S) \to \gamma\eta'; \eta \to \pi^+\pi^-\pi^0$.

D. The Decay $\Upsilon \to \gamma\eta', \eta' \to \gamma\rho^0$

The reconstruction scheme for the decay chain $\Upsilon(1S) \to \gamma\eta'$; $\eta' \to \gamma\rho^0$ is slightly different from those previously described. We first build ρ^0 candidates by forcing pairs of oppositely

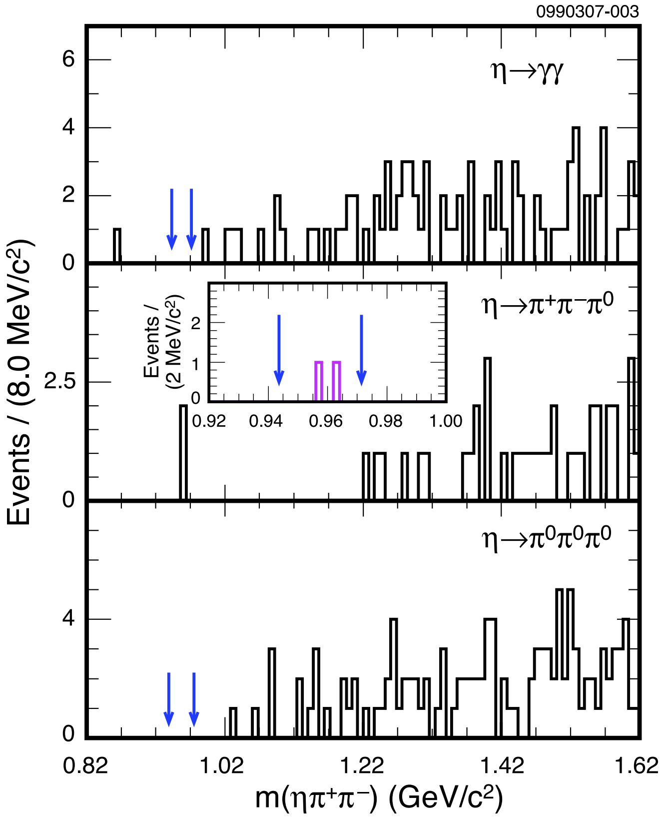

FIG. 3: Invariant mass distributions of $\eta\pi^+\pi^-$ candidates from Υ(1S) data. The η candidate is constrained to the nominal η meson mass. No events are observed in the signal box for $\eta \to \gamma\gamma$ (top) and $\eta \to \pi^0\pi^0\pi^0$ (bottom); two signal events are observed for $\eta \to \pi^+\pi^-\pi^0$ (middle).

charged tracks to originate from a common vertex. Next, we add a photon candidate (which we refer to as the "soft shower" having energy E_s in contrast with the high energy radiative photon) not associated with charged tracks, and having a lateral profile consistent with being a photon, to build η' candidates. To obtain the maximum yield, we neither restrict the energy E_s of the photon nor the invariant mass of the ρ^0 candidate at this stage. A high energy photon is then added, ensuring that the soft shower and high energy photon are distinct, to build the Υ candidate. The Υ candidate is then constrained to the 4-momentum of the initial e^+e^- system and the candidate with the lowest $\chi^2_{\rm P4}$ value is selected.

The candidate η' invariant mass resolution is vastly improved due to the mass-constraints on the candidate π^0 and η mesons in $\eta' \to \eta\pi^+\pi^-$ decays. In reconstruction of $\eta' \to \gamma\rho^0$, a significant improvement in candidate η' invariant mass resolution ($\approx 30\%$) as well as the energy resolution of the soft shower is achieved by performing the 4-momentum constraint on the Υ candidate.

Particle identification in the channel $\eta' \to \gamma\rho^0$ is achieved by demanding the combined RICH and dE/dx likelihood for the pion hypothesis be greater than the combined likelihood for each of the electron, kaon and proton hypotheses. Copiously produced QED processes such as $e^+e^- \to \gamma\gamma e^+e^-$ are suppressed by imposing an electron veto, requiring that $|E/p - 1.0| > 0.05$, where p is the measured momentum and E is the associated calorimeter energy of the charged track. QED events of the type $e^+e^- \to \gamma\gamma\mu^+\mu^-$ are suppressed by requiring that neither track registers a hit five hadronic interaction lengths deep into the muon detector

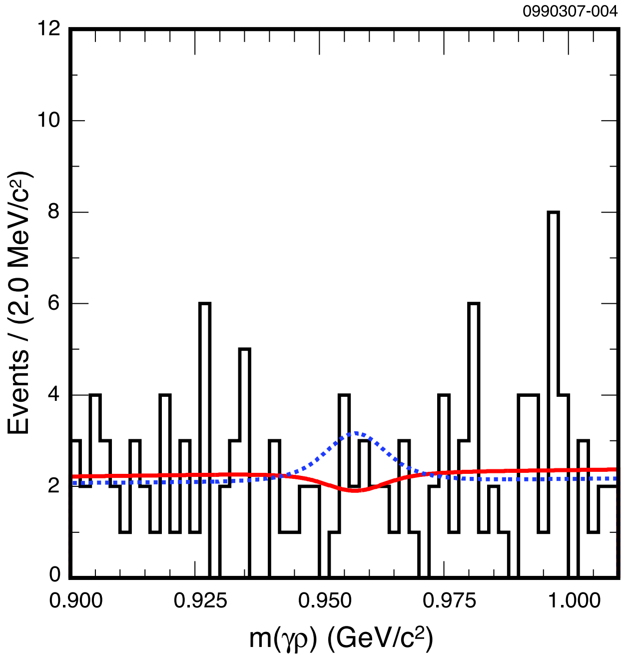

FIG. 4: Invariant mass distribution of $\gamma\rho^0$ candidates in $\Upsilon(1S)$ data for the mode $\Upsilon(1S) \to \gamma\eta'$; $\eta' \to \gamma\rho^0$ overlaid with fits using a) floating area (solid red) yielding -3.1 ± 5.3 events, and b) area fixed to 8.6 events (dashed blue), corresponding to the upper limit at 90% C.L.

system. Continuum background of the type $e^+e^- \to \gamma\gamma\rho^0$ is suppressed by demanding $E_s > 100$ MeV. Finally, the event is ensured to be complete by demanding $\chi^2_{\mathrm{P4}} < 100$. The overall efficiency of the selection criteria for this mode is $(40.1 \pm 2.1)\%$, including possible systematic uncertainties and the statistical uncertainty of the Monte Carlo sample.

Although highly efficient, our selection criteria are not sufficient to suppress the smooth continuum background from the reaction $e^+e^- \to \gamma\gamma\rho^0$. The candidate $\eta' \to \gamma\rho^0$ invariant mass distribution after our selection criteria, shown in Figure 4, is fit to a double Gaussian function over a floating polynomial background function of order one. The parameters of the double Gaussian function are fixed to the values obtained from a fit to signal Monte Carlo and the area is left to float. The likelihood fit yields -3.1 ± 5.3 events, which is consistent with zero. In the absence of a clear signal, we determine the upper limit yield as we do in the case of $\Upsilon(1S) \to \gamma\eta; \eta \to \gamma\gamma$, and find an upper limit at 90% confidence level of 8.6 events.

IV. SYSTEMATIC UNCERTAINTIES AND COMBINED UPPER LIMITS

Since we do not have a signal in any of the modes, and since the kinematic efficiency is near-maximal, statistical uncertainties dominate over systematic uncertainties. By comparison of the expected yield of the QED process $e^+e^- \to \gamma\gamma\gamma$ with the calculated cross-section for this process, we estimate the uncertainty on the trigger simulation for "all neutral" modes to be 4.5%. For modes with only two charged tracks, we have studied the QED processes $e^+e^- \to \gamma\rho^0$ and $e^+e^- \to \gamma\phi$, and assign a 13% uncertainty on the efficiency due to possible trigger mismodeling. For events with many charged tracks, we assign a systematic

TABLE I: Contributions to systematic uncertainties in the efficiencies for $\Upsilon(1S) \to \gamma\eta'$ (upper half) and $\Upsilon(1S) \to \gamma\eta$ (lower half). The uncertainties are expressed as relative percentages and combined in quadrature.

Uncertainty source	$\eta'; \eta \to \gamma\gamma$	$\eta'; \eta \to \pi^+\pi^-\pi^0$	$\eta'; \eta \to \pi^0\pi^0\pi^0$	$\eta' \to \gamma\rho^0$
Trigger mismodeling	13	1	13	1
Track reconstruction	2	4	2	2
Calorimeter response	5	5	15	2.5
Analysis cuts	4	5.7	4	3.9
Monte Carlo statistics	1.0	1.6	2.4	1.0
Combined uncertainty	14.7	8.8	20.4	5.2
Uncertainty source	$\eta \to \gamma\gamma$	$\eta \to \pi^+\pi^-\pi^0$	$\eta \to \pi^0\pi^0\pi^0$	
Trigger mismodeling	4.5	13	4.5	
Track reconstruction	-	2	-	
Calorimeter response	5	5	15	
Analysis cuts	7	4	-	
Monte Carlo statistics	1.3	1.2	1.7	
Combined uncertainty	9.8	15.2	16.0	

uncertainty of 1% as the relevant trigger lines are very well understood, redundant, and very efficient. We assign 1% uncertainty per track in charged track reconstruction based upon CLEO studies [15] of low-multiplicity events, and 2.5% systematic uncertainty per photon from mismodeling of calorimeter response which translates to 5% uncertainty per meson (π^0 and η) decaying into $\gamma\gamma$, again based upon CLEO studies [15]. The systematic uncertainty in $\mathrm{S}_{dE/dx}$ for two tracks added in quadrature (as in $\Upsilon(1S) \to \gamma\eta; \eta \to \pi^+\pi^-\pi^0$) was evaluated to be 4% by considering the efficiency difference of this requirement in Monte Carlo and data samples of $e^+e^- \to \gamma\omega$. Consequently, we assign 4% and 5.7% uncertainty to the reconstruction efficiencies of modes involving two and four charged tracks, respectively, excepting $\eta' \to \gamma\rho^0$ where this requirement was not imposed. For the mode $\eta' \to \gamma\rho^0$, the systematic uncertainty in the efficiency of analysis cuts, found to be 3.9%, was evaluated by comparing the efficiency difference in Monte Carlo and data by studying the ρ^0 signal due to the QED processes. For the neural-net cut in the mode $\Upsilon(1S) \to \gamma\eta; \eta \to \gamma\gamma$, we studied the efficiency in QED $e^+e^- \to \gamma\gamma\gamma$ simulated events and the real data dominated by the same QED process for a wide range of neural-net output values. We find a maximum difference of 7% in these two numbers, which we take as a conservative estimate of the associated systematic uncertainty. The systematic uncertainties for various η and η' decay modes are listed in Table I. These uncertainties were added in quadrature, along with the statistical error due to the limited size of Monte Carlo samples, to obtain the overall systematic uncertainties in the efficiencies.

The systematic uncertainties in efficiencies, uncertainties in the product branching ratios, and the statistical uncertainty in the number of $\Upsilon(1S)$ decays, $N_{\Upsilon(1S)}$, are incorporated [16] by a "toy" Monte Carlo procedure to obtain smeared likelihood distributions for the branching fraction in each mode, $\mathcal{B}(\Upsilon(1S) \to \gamma\mathrm{P}) = N_{\mathrm{P}}/(\epsilon_i \cdot \mathcal{B}_{\mathrm{P},i} \cdot N_{\Upsilon(1S)})$, where $\mathrm{P} = \eta, \eta'$, and ϵ_i and $\mathcal{B}_{\mathrm{P},i}$ denote the efficiency and branching fractions of the ith mode. To obtain the smeared likelihood distribution $\mathcal{L}_{\mathrm{P},i}$, the experiment is performed multiple times, randomly selecting N_{P} from the likelihood function appropriate for each mode[2] and then dividing by

[2] For modes with zero or few observed events, the appropriate likelihood function is generated from Poisson statistics. For the background limited modes $\eta \to \gamma\gamma$ and $\eta' \to \gamma\rho^0$, we already have the likelihood

TABLE II: Results of the search for $\Upsilon(1S) \to \gamma\eta'$ and $\Upsilon(1S) \to \gamma\eta$. Results include statistical and systematic uncertainties, as described in the text. The combined limit is obtained after including the systematic uncertainties.

	$\eta';\eta \to \gamma\gamma$	$\eta';\eta \to \pi^+\pi^-\pi^0$	$\eta';\eta \to \pi^0\pi^0\pi^0$	$\eta' \to \gamma\rho^0$
Observed events	0	2	0	-3.1 ± 5.3
$\mathcal{B}_{\eta',i}\%$	17.5 ± 0.6	10.0 ± 0.4	14.4 ± 0.5	29.5 ± 1.0
Reconstruction efficiency (%)	35.2 ± 5.2	24.5 ± 2.2	14.4 ± 2.9	40.1 ± 2.1
$\mathcal{B}(\Upsilon(1S) \to \gamma\eta')$(90% C.L.)[a]	$< 1.8 \times 10^{-6}$	$< 10.3 \times 10^{-6}$	$< 5.2 \times 10^{-6}$	$< 3.4 \times 10^{-6}$
$\mathcal{B}(\Upsilon(1S) \to \gamma\eta')$(90% C.L.)[b]	$< 1.9 \times 10^{-6}$	$< 10.4 \times 10^{-6}$	$< 5.8 \times 10^{-6}$	$< 3.4 \times 10^{-6}$
Combined limit on $\mathcal{B}(\Upsilon(1S) \to \gamma\eta')$		$< 1.9 \times 10^{-6}$		

	$\eta \to \gamma\gamma$	$\eta \to \pi^+\pi^-\pi^0$	$\eta \to \pi^0\pi^0\pi^0$
Observed events	-2.3 ± 8.7	0	0
$\mathcal{B}_{\eta,i}\%$	39.4 ± 0.3	22.6 ± 0.4	32.5 ± 0.3
Reconstruction efficiency (%)	23.8 ± 2.4	28.5 ± 2.9	11.8 ± 1.9
$\mathcal{B}(\Upsilon(1S) \to \gamma\eta)$(90% C.L.)[a]	$< 7.3 \times 10^{-6}$	$< 1.7 \times 10^{-6}$	$< 2.8 \times 10^{-6}$
$\mathcal{B}(\Upsilon(1S) \to \gamma\eta)$(90% C.L.)[b]	$< 7.4 \times 10^{-6}$	$< 1.8 \times 10^{-6}$	$< 2.9 \times 10^{-6}$
Combined limit on $\mathcal{B}(\Upsilon(1S) \to \gamma\eta)$		$< 1.0 \times 10^{-6}$	

[a]excluding systematic uncertainties
[b]including systematic uncertainties

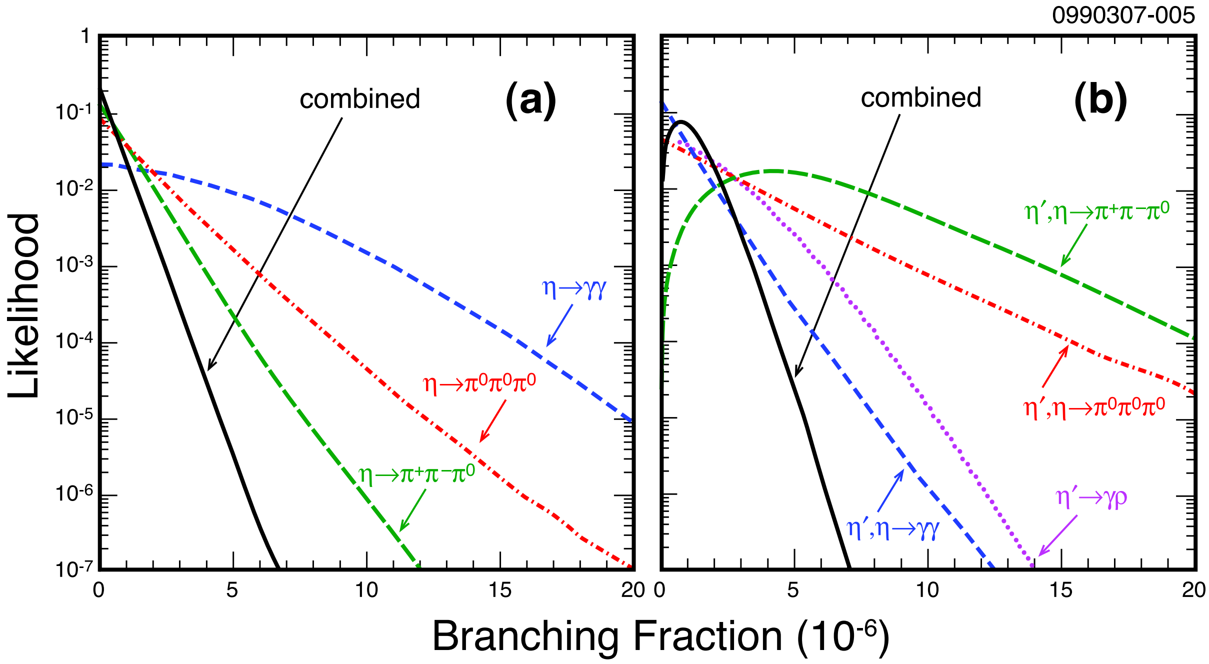

FIG. 5: Likelihood distributions as a function of branching fraction for the decay mode $\Upsilon(1S) \to \gamma\eta$ (left) and $\Upsilon(1S) \to \gamma\eta'$ (right). All distributions are smeared by respective systematic uncertainties and normalized to the same area. The solid black curve denotes the combined likelihood distribution.

the sensitivity factor $\epsilon_i \cdot \mathcal{B}_{P,i} \cdot N_{\Upsilon(1S)}$, where each term is picked from a Gaussian distribution about their mean values with the appropriate standard deviation.

function which we used in calculating the upper limit of the observed number of events at 90% CL.

The combined likelihood distribution for $\mathcal{B}(\Upsilon(1S) \to \gamma P)$ is derived as $\mathcal{L}_P = \prod_i \mathcal{L}_{P,i}$ which is summed up to 90% of the area in the physically allowed region to obtain the upper limit branching fraction for $\Upsilon(1S) \to \gamma P$. From the constituent $\mathcal{L}_{P,i}$ and the combined $\mathcal{L}_P$ as shown in Figure 5, we obtain upper limits on $\mathcal{B}(\Upsilon(1S) \to \gamma\eta)$ of 7.4×10^{-6}, 1.8×10^{-6}, 2.9×10^{-6}, and 1.0×10^{-6} for η decaying into $\gamma\gamma$, $\pi^+\pi^-\pi^0$, $\pi^0\pi^0\pi^0$, and all three combined, respectively. We obtain upper limits for $\mathcal{B}(\Upsilon(1S) \to \gamma\eta')$ of 1.9×10^{-6}, 10.4×10^{-6}, 5.8×10^{-6}, and 3.4×10^{-6} for η decaying into $\gamma\gamma$, $\pi^+\pi^-\pi^0$, $\pi^0\pi^0\pi^0$, and $\eta' \to \gamma\rho^0$, respectively. The combined upper limit for $\mathcal{B}(\Upsilon(1S) \to \gamma\eta')$ is 1.9×10^{-6}, a value larger than one of the sub-modes ($\Upsilon(1S) \to \gamma\eta'; \eta \to \gamma\gamma$), due to the two candidate events in $\Upsilon(1S) \to \gamma\eta'; \eta \to \pi^+\pi^-\pi^0$. The numbers of observed events, detection efficiencies and upper limits are listed in Table II.

V. SUMMARY AND CONCLUSION

We report on a new search for the radiative decay of $\Upsilon(1S)$ to the pseudoscalar mesons η and η' in 21.2×10^6 $\Upsilon(1S)$ decays collected with the CLEO III detector. The η meson was reconstructed in the three modes $\eta \to \gamma\gamma$, $\eta \to \pi^+\pi^-\pi^0$ or $\eta \to \pi^0\pi^0\pi^0$. The η' meson was reconstructed either in the mode $\eta' \to \gamma\rho^0$ or $\eta' \to \pi^+\pi^-\eta$ with η decaying through any of the above three modes. All these modes except for $\eta' \to \gamma\rho^0$ had earlier been investigated in CLEO II data amounting to $N_{\Upsilon(1S)} = 1.45 \times 10^6$ $\Upsilon(1S)$ mesons and resulted in previous upper limits $\mathcal{B}(\Upsilon(1S) \to \gamma\eta') < 1.6 \times 10^{-5}$ and $\mathcal{B}(\Upsilon(1S) \to \gamma\eta) < 2.1 \times 10^{-5}$ at 90% C.L. These limits were already smaller than the naive predictions based upon the scaling of the decay rate for the corresponding J/ψ radiative decay mode by the factor $(q_b m_c/q_c m_b)^2$, and also the model of Körner *et al.,* [17], whose perturbative QCD approach predictions for $\mathcal{B}(J/\psi \to \gamma X)$ where $X = \eta, \eta', f_2$ as well as $\mathcal{B}(\Upsilon(1S) \to \gamma f_2)$ agree with experimental results.

With a CLEO III data sample 14.6 times as large as the CLEO II data sample, we find no convincing signal in any of the modes. Based purely upon the luminosities, we would expect the new upper limits to be scaled down by a factor of between 14.6 (in background-free modes) and $\sqrt{14.6}$ in background dominated modes if the two CLEO detectors (CLEO II and CLEO III) offered similar particle detection efficiencies. In the search for $\Upsilon(1S) \to \gamma\eta$ we find no hint of a signal, and manage to reduce the limit by an even larger factor. In the search for $\Upsilon(1S) \to \gamma\eta'$, however, we find two clean candidate events in the channel $\Upsilon(1S) \to \gamma\eta'; \eta \to \pi^+\pi^-\pi^0$, which, though we cannot claim them as signal, do indicate the possibility that we are close to the sensitivity necessary to obtain a positive result. Because of these two events, our combined limit for $\Upsilon(1S) \to \gamma\eta'$ is not reduced by as large a factor as the luminosity ratio, and in fact is looser than that which would be obtained if we analyzed one sub-mode ($\Upsilon(1S) \to \gamma\eta'; \eta \to \gamma\gamma$) alone. In this analysis we found upper limits which we report at 90% confidence level as

$$\mathcal{B}(\Upsilon(1S) \to \gamma\eta) < 1.0 \times 10^{-6},$$

$$\mathcal{B}(\Upsilon(1S) \to \gamma\eta') < 1.9 \times 10^{-6}.$$

Our results are sensitive enough to test the appropriateness of the pseudoscalar mixing approach as pursued by Chao [8], where mixing angles among various pseudoscalars including η_b are calculated. Then, using a calculation for the M1 transition $\Upsilon \to \gamma\eta_b$, he predicts

$\mathcal{B}(\Upsilon(1S) \to \gamma\eta) = 1 \times 10^{-6}$ and $\mathcal{B}(\Upsilon(1S) \to \gamma\eta') = 6 \times 10^{-5}$. Our limit for $\Upsilon(1S) \to \gamma\eta'$ is significantly smaller than Chao's prediction and does not support his approach.

The sensitivity challenge posed by both the extended vector dominance model and the higher twist approach of Ma are beyond our reach. In extended VDM, Intemann predicts $1.3 \times 10^{-7} < \mathcal{B}(\Upsilon(1S) \to \gamma\eta) < 6.3 \times 10^{-7}$ and $5.3 \times 10^{-7} < \mathcal{B}(\Upsilon(1S) \to \gamma\eta') < 2.5 \times 10^{-6}$, where the two limits are determined by having either destructive or constructive interference, respectively, between the terms involving $\Upsilon(1S)$ and $\Upsilon(2S)$. Even if it is determined that the amplitudes are added constructively, our limit remains higher than the VDM prediction for $\Upsilon(1S) \to \gamma\eta$.

Ma's prediction of $\mathcal{B}(\Upsilon(1S) \to \gamma\eta') \approx 1.7 \times 10^{-6}$ is consistent with our result. However, his prediction for $\mathcal{B}(\Upsilon(1S) \to \gamma\eta) \approx 3.3 \times 10^{-7}$ is a factor of ~ 3 smaller than our limit.

We gratefully acknowledge the effort of the CESR staff in providing us with excellent luminosity and running conditions. D. Cronin-Hennessy and A. Ryd thank the A.P. Sloan Foundation. This work was supported by the National Science Foundation, the U.S. Department of Energy, and the Natural Sciences and Engineering Research Council of Canada.

---

[1] Y.-M. Yao *et al.,* (Particle Data Group), J. Phys. G**33**, 1 (2006).
[2] S. Richichi *et al.,* (CLEO Collaboration), Phys. Rev. Lett. **87**, 141801 (2001).
[3] A. Anastassov *et al.,* (CLEO Collaboration), Phys. Rev. Lett. **82**, 286 (1999).
[4] S. B. Athar *et al.,* (CLEO Collaboration), Phys. Rev. D **73**, 032001 (2006).
[5] D. Besson *et al.,* (CLEO Collaboration), Phys. Rev. D **75**, 072001 (2007).
[6] G. Masek *et al.,* (CLEO Collaboration), Phys. Rev. D **65**, 072002 (2002).
[7] G. W. Intemann, Phys. Rev. D **27** 2755 (1983).
[8] K. T. Chao, Nucl. Phys. **B335**, 101 (1990).
[9] V. N. Baier and A. G. Grozin, Nucl. Phys. **B192**, 476 (1981).
[10] J. P. Ma, Phys. Rev. D **65**, 097506 (2002).
[11] Y. Kubota *et al.,* Nucl. Instrum. Methods Phys. Res., Sect. A **320**, 66 (1992); G. Viehhauser *et al.,* Nucl. Instrum. Methods Phys. Res., Sect. A **462**, 146 (2001); D. Peterson *et al.,* Nucl. Instrum. Methods Phys. Res., Sect. A **478**, 142 (2002); A. Warburton *et al.,* Nucl. Instrum. Methods Phys. Res., Sect. A **488**, 451 (2002); M. Artuso *et al.,* Nucl. Instrum. Methods Phys. Res., Sect. A **502**, 91 (2003); **554**, 147 (2005).
[12] R. A. Briere *et al.,* (CLEO Collaboration), Phys. Rev. D **70** 072001 (2004).
[13] R. Brun *et al.*, GEANT 3.21, CERN Program Library Long Writeup W5013 1993 (unpublished).
[14] M. A. Selen, R. M. Hans, and M. J. Haney, IEEE Trans. Nucl. Sci. **48**, 562 (2001).
[15] S. A. Dytman *et al.,* (CLEO Collaboration), hep-ex/0307035.
[16] R. D. Cousins and V. L. Highland, Nucl. Instrum. Methods Phys. Res., Sect. A **320**, 331 (1992).
[17] J. G. Körner, J. H. Kühn, M. Krammer, H. Schneider, Nuclear Physics **B229**, 115 (1983).